Modelling quasar accretion disks from Hα emission

Emily Down, Oxford Astrophysics - Steve Rawlings, Oxford Astrophysics
Devinder Sivia, St John's College, Oxford - Jo Baker, formerly Oxford Astrophysics

1. Structure of accretion disks

Active Galactic Nuclei (AGN) are powered by accretion of gas and dust onto supermassive black holes. As the black hole feeds on the surrounding material, this forms an accretion disk of infalling matter (Shakura & Sunyaev, 1973). The model considered includes a thick, hot inner disk which shields and reprocesses the hard X-ray emission from the black hole (Rees et al., 1982), and a flattened, extended outer disk which is optically thick. The outer disk, which can extend from $\sim 10^2$ to 10^5 gravitational radii, emits excess UV continuum emission, which is seen in the form of the "Big Blue Bump", and which gives rise to the Baldwin Effect, an anticorrelation between UV continuum luminosity and the equivalent widths of CIV (Netzer, 1985). The strongest argument for the presence of accretion disks are the double-peaked lines observed in some AGN.

2. Double-peaked optical emission

A range of distinctive line profiles may arise from a thin, rotating, circular accretion disk. The approaching material is redshifted, and the receding material blueshifted, such that when the disk is tilted at a significant angle to the line of sight, the emission is double peaked. The blueshifted peak is of higher intensity than the redshifted peak due to Doppler boosting. Even more complex line profiles are possible, e.g. from elliptical disks (Gurzadyan & Ozernoy, 1979), or warped disks which are linked to rotating black holes (Bachev, 1999).

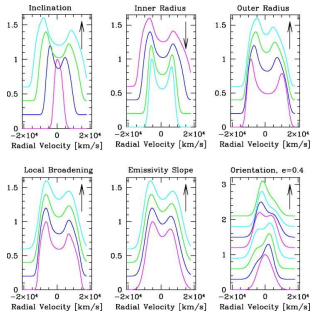

Fig 1: Partial figure from Strateva et al. (2003) showing the strong dependence of the line profile of the angle of the accretion disk.

Double-peaked emission has been seen in a relatively low fraction of AGN to date. Strateva et al. (2003) found that ~3% of the SDSS AGN (including radio-quiet and radio-loud) showed obvious double-peaked lines, while Eracleous et al. (2003) found these profiles in ~20% of their sample of radio-loud sources.

The emission profile arising from a rotating circular accretion disk depends on the inner and outer radii of the disk, on the local velocity dispersion of the material, on the disk emissivity, and on the angle of the disk to the line of sight. As shown in Figure 1 (Strateva et al., 2003), the separation of the line peaks is most strongly dependent on the angle of the disk. Disks at smaller angles may not be double-peaked.

3. Modelling quasar orientation from Hα emission

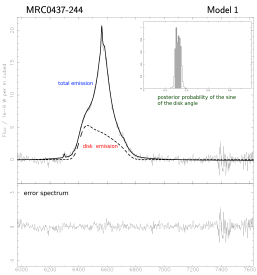

Fig 2: Example fit of a composite emission model to the IR spectrum of the quasar MRC0437-244.

A sub-sample of 19 high-z ($0.8 < z < 2.3$) radio-loud quasars from the Molonglo Quasar Sample were observed in the near-IR using ISAAC at the VLT. The Hα emission lines were fitted with a range of composite emission models, using BayeSys3 by John Skilling (http://www.inference.phy.cam.ac.uk/bayesys), a Bayesian statistical Monte Carlo engine.

Emission-line models included combinations of:
❋ Accretion disk emission, following the calculations of Chen & Halpern (1989).
❋ Either Lorentzian or Gaussian single-peaked broad lines, which could arise in a disk wind or from fast-moving clouds outside the disk.
❋ Narrow lines with Gaussian profiles.

The model with the highest Bayesian evidence was selected, and the angle of the accretion disk to the line of sight was obtained from this model. An example fit is shown in Figure 2. It should be noted that for models with similar Bayesian evidence, the disk angles were consistent.

All but one of the 19 quasars were found to have strong Bayesian evidence for broad emission consisting of at least two components. 10/19 quasars showed strong Bayesian evidence for a component of accretion disk emission, with a further 8 consistent with the presence of a disk. Only one quasar had evidence against a disk: this object displays complex broad Hα emission with at least 3 components. The fact that the disk emission appears to arise together with a second, single-peaked line may explain why so few AGN are observed to have strongly double-peaked line profiles.

A correlation was found between the linear sizes of the quasars on the sky and the disk angles, with a probability of 74% by Kendall's Tau. This is consistent with the expected geometric projection effect for a sample of sources expanding linearly up to a cut-off size of ~1 Mpc.

4. Velocity shifts of the emission regions

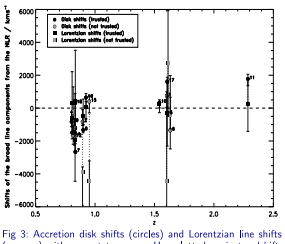

Fig 3: Accretion disk shifts (circles) and Lorentzian line shifts (squares) with respect to narrow Hα, plotted against redshift.

The broad line components were allowed to shift by ± 4500 kms^{-1} compared to the narrow line region (NLR). For 7/16 of sources with reliable redshifts, the velocity shifts were not trusted, as the parameters representing broad or narrow Hα were fitting to a different component of emission. For the remaining 9 cases, the broad line material is generally blueshifted with respect to the narrow lines, in agreement with the majority of the literature: average velocity shifts were -180 kms^{-1} for the accretion disks and -240 kms^{-1} for the Lorentzian lines. If dust in the plane of the AGN obscures the far-side emission from view, this indicates outflows of the broad-line emitting material relative to a stationary NLR.

Separating by redshift, 6/9 Lorentzian lines with $z < 1$ have an average blueshift of -380 kms^{-1}, whereas the 3/9 with $z > 1$ have an average shift of $+40$ kms^{-1}, so the single-peaked emission is consistent with a region of similar velocity to the NLR. However, the low-z and high-z disk emission has average shifts of -890 kms^{-1} and $+620$ kms^{-1} respectively. Figure 3 illustrates this possible correlation between the disk shift and the redshift, significant at 2 σ. This may result from the dependence of both of these quantities on the optical or radio luminosity (z-dependence on luminosity arises because sources at greater distances are more powerful).

The measured velocity shifts imply that the single-peaked lines arise from a region with a similar velocity to the NLR. If the accretion disks are at the systemic velocity, then the narrow lines are inflowing for low-redshift sources, and outflowing from the higher-redshift, more luminous sources.

The entire analysis was repeated with the disk fixed at the systemic velocity, as given by the narrow lines, and the results were consistent with those given here.

4. Receding torus model

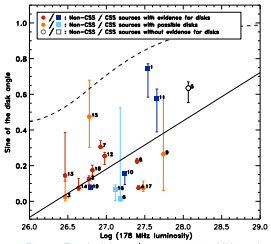

Fig 4: Fitted disk angles versus 178 MHz radio luminosity. The solid line is the best-fit line. The dotted line shows the calculated critical angle following Willott et al. (2000), with fiducial angle 45° at log $L_{178\ MHz}$ = 27, and minimum quasar fraction 10%.

The receding torus model postulates that more luminous sources have larger opening angles of their dusty torus, and hence the broad lines of a quasar can be seen up to a larger viewing angle (Lawrence, 1991). Simpson (1998) proposed that this may be due to dust sublimation proportional to the source luminosity. The prediction of this model is therefore that the more luminous quasars will have jet angles ranging up to a higher cut-off value.

There is a weak correlation between the best-fit disk angles and the low-frequency radio luminosity (Figure 4) at a probability of 93% according to Kendall's Tau test. The measurement of the disk angle is independent of radio luminosity, and so the correlation between these parameters gives direct, albeit weak, evidence for the receding torus model in which the disks are aligned along the same axes as the jets, if it is assumed that the disks are perpendicular to the jet axis.

5. Orientation of quasars

AGN have at most one axis of symmetry, and it is therefore necessary to carefully consider orientation effects. There are two types of orientation effects which occur: obscuration by a screen of matter, such as a dusty molecular torus; and Doppler boosting of radiation arising from the relativistic plasma jets. As the radio lobes are extended, the low-frequency emission from these is similarly visible from most viewing angles. However, when viewed at angles close to the radio jet, the core of the quasar is Doppler-boosted, and much more luminous than when viewed at large angles. The ratio between the core flux and the lobe flux of a radio source therefore gives an orientation measure.

6. Modelling quasar orientation from radio SEDs

Radio spectral energy distributions of the total flux densities over the range 10 MHz to 20 GHz were assembled from a variety of sources, together with core flux densities, which were assumed to be constant across all radio frequencies. These were fitted using BayeSys3 with a model which calculated the core-to-lobe flux ratio, and translated this directly into a jet angle. This was achieved by normalising the Molonglo quasar sub-sample, which was selected at 408 MHz and therefore suffers from contamination by quasars boosted into the sample by their strong cores (2/19 sources), by the 3CRR sample, which is assumed to consist of AGN oriented randomly in space. An example model fit is shown in Figure 5.

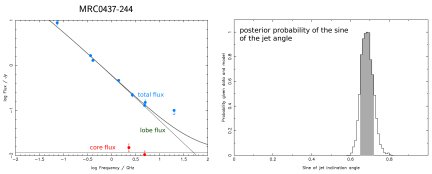

Fig 5: Example fit to the SED of quasar MRC0437-244.

7. What triggers radio jets?

The majority of powerful AGN are found in elliptical galaxies, which are believed to form in galaxy mergers (Barnes & Hernquist, 1991). It is therefore plausible that the radio jets might be triggered by mergers, which provide a fresh reservoir of gas to fuel the black hole (Scheuer, 1992). In the wake of a merger, the outer accretion disk may be offset from the black hole spin, while the inner disk will be aligned via the Lense-Thirring effect. Since radio jets are thought to be launched along the spin axis of the black hole (Blandford & Znajek, 1977), this could result in a misalignment between the accretion disk and the radio jets. This effect would correct itself over a timescale of $\sim 10^7$ - 10^8 years, as the black hole is spun up by the accretion disk (Scheuer & Feiler, 1996).

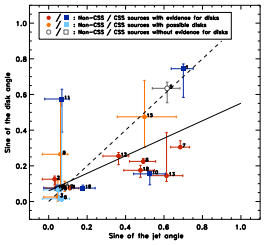

Fig 6: Fitted disk angles vs. fitted jet angles. The solid line is the best-fit line, and the dotted line marks where the disk angle is equal to the jet angle.

Figure 6 shows disk angles fitted from the Hα emission plotted against jet angles fitted from radio spectral energy distributions. There is a correlation between these independently-measured angles at a significance of >99% by Kendall's Tau. To a first approximation, the accretion disks and radio jets appear to be orthogonal. The outlier on this plot (quasar 11) is a Compact Steep Spectrum object (CSS); these quasars have the characteristics of sources viewed at a large angle to their radio jets despite a small angular size in the sky, and so these are thought to be young AGN. It is possible that this source has a misaligned disk and jet caused by a galaxy merger which triggered the activity, but without better statistics, this is just speculation.

8. Summary

❋ 10/19 sources have strong evidence for a component of accretion disk emission, 18/19 sources are consistent with the presence of a disk. Complex emission models are required.
❋ A possible redshift-dependent velocity offset between the narrow line region and the accretion disk is found. See Down et al. (MNRAS, 401, 633, 2010) for details.
❋ The angle of the accretion disk to the line of sight is weakly correlated with low-frequency radio luminosity, in support of the receding torus model. Opening angles are consistent with this model.
❋ Independently-measured accretion disk and radio jet angles are correlated, i.e. there is no strong evidence for misaligned jets and disks in this sample.

References:

Shakura & Sunyaev, 1973, *AA*, 24, 337 ❋ Rees et al., 1982, *Nature*, 295, 17 ❋ Netzer, 1985, *MNRAS*, 216, 63 ❋ Gurzadyan & Ozernoy, 1979, *Nature*, 280, 214 ❋ Bachev, 1999 *A&A*, 348, 71 ❋ Strateva et al., 2003, *AJ*, 126, 1720 ❋ Eracleous & Halpern, 2003, *ApJ*, 599, 886 ❋ Chen et al., 1989, *ApJ*, 339, 742 ❋ Lawrence, 1991, *MNRAS*, 252, 586 ❋ Simpson, 1998, *MNRAS*, 297, L39 ❋ Willott et al., 2000, *MNRAS*, 316, 449 ❋ Barnes & Hernquist, 1991, *ApJ*, 370, L65 ❋ Scheuer, 1992, *Proc. 7th IAP Meeting* ❋ Blandford & Znajek, 1977, *MNRAS*, 179, 433 ❋ Scheuer & Feiler, 1996, *MNRAS*, 282, 291